Glass and bioglass nanopowders by flame synthesis†

Tobias J. Brunner, Robert N. Grass and Wendelin J. Stark*

Received (in Cambridge, UK) 12th December 2005, Accepted 6th February 2006
First published as an Advance Article on the web 21st February 2006
DOI: 10.1039/b517501a

The preparation of amorphous nanopowders by flame synthesis opens access to common soda-lime, metal-doped glasses or bioglasses in the range of 20–80 nm and offers an alternative to conventional wet-phase preparation, solid state reactions or melting.

Glasses and glass ceramics consist of undercooled, partially or fully amorphous materials. For thousands of years they have been broadly used for their intriguing properties[1,2] including elasticity,[3] transparency,[4] and chemical resistance,[5] and today they are workhorses in data transmission.[6–8] In medicine, certain glass compositions (SiO_2–CaO–P_2O_5–Na_2O) were even found to form tight bonds to living human bone and are applied in a variety of bone grafts for bone repair and regeneration of defects arising from trauma, tumour and osteoporosis.[9–12] Traditionally, oxide-based glasses have been derived by melting of the corresponding oxides at elevated temperatures[13] and result in dense or low-porosity texture materials. The application of complex glasses as nanomaterials would stimulate the development of applications using their intriguing bulk properties at small scale applications. Consequently, sol–gel processes have enabled production of some glasses[14–18] and have resulted in porous structures with high specific surface areas. Low temperature preparations, however, can be limiting in terms of composition,[14] high remaining water or solvent content after synthesis and generally require the use of an annealing or sintering step after preparation.[17,18] The latter inherently promotes the formation of hard agglomerates of the desired glass nanoparticles. We therefore would like to show that the direct preparation of glass nanoparticles in a high temperature environment offers distinct advantages in terms of accessible compositions, homogeneity and particle size.

In order to illustrate the preparation of complex glasses by flame synthesis we prepared commonly used soda-lime and borosilicate glasses (Table 1) and cobalt or gold doped soda lime glass (Fig. 1).[21] In order to extend the range of accessible compositions for high-surface bioglasses we included the preparation of several silica-based bioglasses, optionally doped with fluoride.

Each particular glass was synthesized by combining and mixing corresponding liquid metal and suitable anion precursors and feeding the mixture into a flame reactor.[22] The nanopowders were collected on a filter mounted above the flame. Transmission electron microscopy (TEM) of as-synthesised materials revealed particles of about 20 to 80 nm size (Fig. 1) with specific surface areas from 70 to 90 $m^2\ g^{-1}$ (soda-lime, borosilicate glass and 45S5) and 200 $m^2\ g^{-1}$ (77S). Soda-lime glass doped with cobalt (1.8 wt%) and gold (0.6 wt%) resulted in an intensive colouring of the glass best visible in pressed tablets as shown in Fig. 1. The blue colour of the cobalt doped glass is typical for cobalt(II) introduced into the glass matrix[23,24] and the burgundy colour results from metallic gold doping.[21,25] The chemical composition (Table 1) and homogeneity of the glasses were verified by laser ablation inductively coupled plasma mass spectrometry (LA-ICP-MS) by probing at least 8 times consecutively the same spot on a pressed tablet resulting in a composition depth profile (see ESI†). The formation of glasses was confirmed by the absence of reflections in X-ray powder diffraction (XRD) patterns of all as-synthesised powders (Fig. 2). The calcination of a representative glass (Bioglass 45S5) was followed by thermal analysis coupled to a mass spectrometer (Fig. 3) and by measuring the X-ray diffraction pattern after exposure to temperatures before (pattern 1) and after the corresponding exothermal event at 630 °C (patterns 2 and 3). The initial endothermic peak could be attributed to the desorption

Table 1 Composition of glasses synthesised by flame spray synthesis (in wt%) as measured by laser ablation-ICP-MS

	SiO_2	CaO	Na_2O	P_2O_5	B_2O_3	F[a]
Soda-lime glass	74.3	11.8	14			
Borosilicate glass	58.7	20.4	12.8		8.1	
Bioglass 45S5	47.8	25.1	22.6	4.6		
Bioglass 45S5F	45.4	26.6	21.4	4.3		2.4
Bioglass 77S	79.9	16.8		3.2		

[a] Nominal composition by introducing fluorobenzene as fluorine source.[19,20]

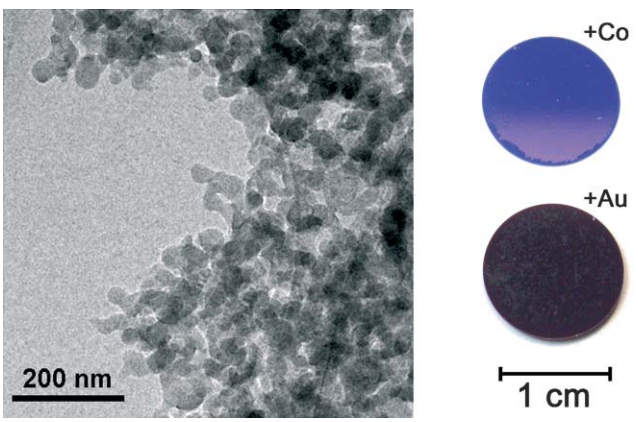

Fig. 1 Transmission electron microscopy image of a flame-made, nanoparticulate Bioglass 45S5 sample showing a high degree of agglomeration (left). Photographs of pressed soda-lime glass doped with cobalt ions or gold displays bright-coloured glasses (right).

Institute for Chemical and Bioengineering, ETH Zurich, HCI E 107, CH-8093 Zürich, Switzerland. E-mail: wendelin.stark@chem.ethz.ch; Fax: +41 44 633 10 83; Tel: +41 44 632 09 80
† Electronic supplementary information (ESI) available: additional XRD pattern, electron micrographs, pore size distributions, UV-VIS spectra and chemical compositions. See DOI: 10.1039/b517501a

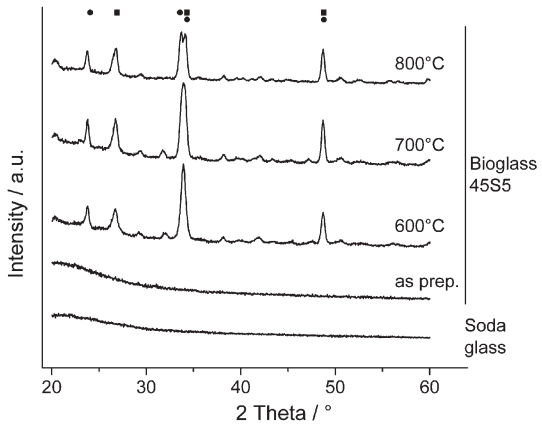

Fig. 2 X-ray diffraction patterns of as-synthesised soda-lime glass and 45S5 Bioglass corroborating the formation of a glass (bottom). Bioglass 45S5 after calcination at different temperatures displays the formation of a glass ceramic phase. (■) $Na_2Ca_2(SiO_3)_3$, (●) $Na_2CaSi_3O_8$.

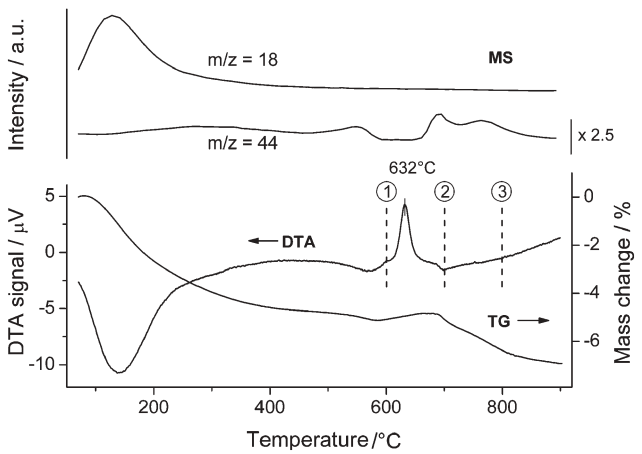

Fig. 3 The calcination of as-prepared bioglass to 800 °C was followed by differential thermal analysis (DTA) and thermogravimetry (TG) and resulted in the evolution of water (m/z = 18) and CO_2 (m/z = 44). X-ray diffraction pattern were taken separately at 600 to 800 °C (numbers 1–3).

of physisorbed water from the surface of the material (MS trace of m/z = 18). The evolution of carbon dioxide (MS trace m/z = 44) showed no prominent decarboxylations and corroborated the stability of the glasses. The XRD pattern indicated that the exothermal peak at 630 °C may be assigned to partial crystallization of the bioglass and formation of a glass ceramic with characteristic peaks for sodium calcium silicates[26] (see Fig. 2).

The development of nano- or microporous glasses has been suggested for nanofiltration,[27] permeable membranes[28] and controlled degradation of biomaterials.[29] The evolution of the pore size distribution during sintering of a representative sample (Bioglass 45S5) was therefore measured by mercury intrusion porosimetry. A pronounced shift in the pore size distribution could be observed with increasing sintering temperature (Fig. 4). As-prepared glass nanopowders exhibited a relatively narrow pore size distribution at 20–60 nm which can be mainly attributed to interparticle pores if compared to the transmission electron micrographs (Fig. 1). At around 500 °C, the material starts to sinter and pores partially collapsed at 550 °C resulting in a bimodal

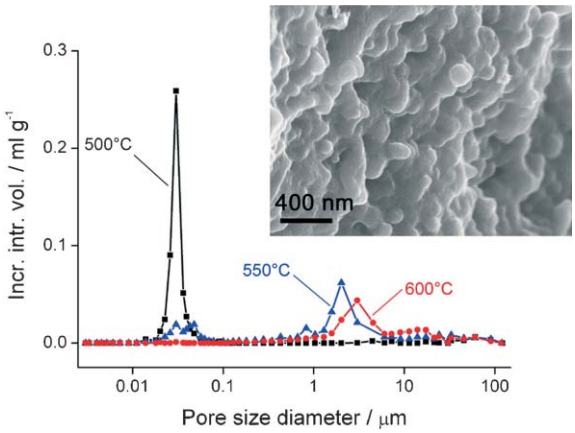

Fig. 4 Mercury intrusion porosimetry of calcined samples of Bioglass 45S5. Inset: Scanning electron micrograph of Bioglass 45S5 after sintering at 600 °C.

pore size distribution with still unaffected pores around 30–60 nm and large pores in the micrometer range. At 600 °C, the smaller pores fully collapsed and the material mainly consists of a microporous glass ceramic (insert, Fig. 4) as evidenced by the XRD pattern. Controlled sintering of glass nanopowders therefore gives access to materials with defined pore sizes.

A bioactive implant material forms an interfacial bond between the implant and the host tissue. Bioactivity of bone implants can be assessed *in vitro* by evaluation of surface reactions in physiological fluids. Bioglass 45S5 was therefore tested by immersion of pressed samples into simulated body fluid (SBF) prepared according to Kokubo *et al.*[30] at 37 °C. After exposure, the surface of the material was investigated by Raman spectroscopy in backscattering mode as suggested by Notingher *et al.*[31] Fig. 5 shows a 45S5 Bioglass sample after 7 days in SBF in comparison to an as-prepared, untreated reference, pure hydroxyapatite[20] and calcium carbonate. The Raman signal at 960 and 1080 cm^{-1} indicated the formation of carbonated hydroxyapatite during immersion in SBF. The same sample investigated under the

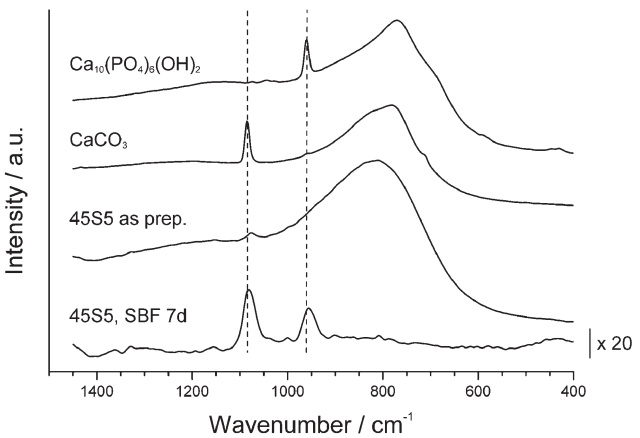

Fig. 5 Raman spectroscopy of bioglass after 7 days in simulated body fluid in comparison to untreated bioglass, calcium carbonate ($CaCO_3$) and hydroxyapatite ($Ca_{10}(PO_4)_6(OH)_2$) are shown. The formation of carbonated hydroxyapatite can be observed.

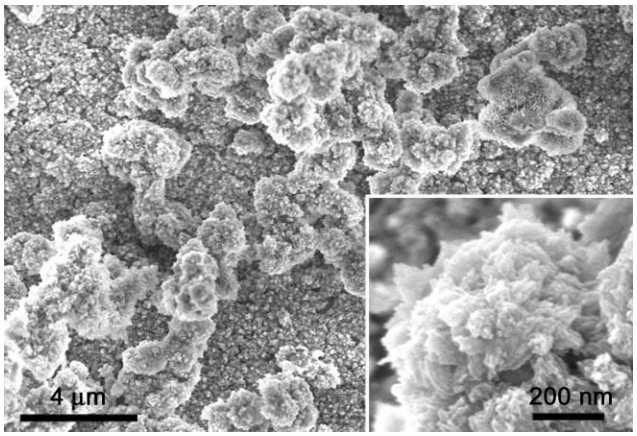

Fig. 6 Scanning electron microscopic image of Bioglass 45S5 after incubation in SBF for 7 days. In contrast to the as-prepared material (Fig. S4, Supplementary Information†), the rough surface is covered by hydroxyapatite crystals as shown by Raman spectroscopy (Fig. 5).

scanning electron microscope (SEM) displays a uniform cover of nanocrystalline apatite (Fig. 6).

In summary, we have shown that highly complex glasses with over five different elements could be readily produced as nanoparticles using a flame reactor. The high temperature synthesis allows preparation of well defined, homogenous amorphous materials and allows doping with transition metal ions or even metals. In order to illustrate one of the many possible complex applications, the preparation of a bioglass was shown to result in a material with controllable pore size and high deposition of bone-like carbonated hydroxyapatite during immersion in simulated body fluid. The results further demonstrate that nanoparticles with highly complex composition are now readily available by a dry, one-step process.‡

We thank F. Krumeich for TEM analyses and D. Günther and K. Hametner for LA-ICP-MS measurements. Financial support by the ResOrtho and the Gebert Rüf Foundation, grant number GRS-048/04, is kindly acknowledged.

Notes and references

‡ Depending on the desired composition, glasses were prepared by flame spray synthesis[22] using 2- ethylhexanoic acid salts of calcium, sodium and cobalt, as well as gold chloride dissolved in acetonitrile, hexamethyldisiloxane (Lancaster), tributyl phosphate (Acros) tributyl borate (Acros) and fluorobenzene (Abcr) as precursors. The liquid mixtures were fed through a capillary (diameter 0.4 mm) into a methane (1.13 l min^{-1}, Pan Gas, tech)/oxygen (2.4 l min^{-1} Pan Gas, tech) flame using a gear-ring pump (HNP Mikrosysteme) at a rate of 5 ml min^{-1}. Oxygen (5 l min^{-1}, Pan Gas, tech, constant pressure drop at the capillary tip 1.5 bar) was used to disperse the liquid leaving the capillary. Calibrated mass flow controllers (Brooks) were used to control all gas flows. The as-formed particles were collected on glass fibre filters (Whatmann GF/A, 25.7 cm in diameter), placed on a cylinder mounted above the flame, by the aid of a vacuum pump (Busch Seco SV 1040 C).

For analysis, specific surface area according to the BET method was obtained on a Micromeritics Tristar. X-ray diffraction was conducted on a Stoe STADI-P2 (Ge monochromator, $CuK_{\alpha 1}$, PSD detector). Element analysis was performed by laser ablation inductively coupled plasma mass spectrometry (LA-ICP-MS).[32] TEM images were recorded on a CM30 ST (Philips, LaB_6 cathode, operated at 300 kV, point resolution ~4 Å). Particles were deposited onto a carbon foil supported grid. SEM analysis was performed on a LEO 1530 Gemini after sputtering the samples with ~4 nm of platinum. Simulated body fluid was prepared according to Kokubo *et al.*[30] and sterile filtered (Nalgene). Mercury intrusion porosimetry was measured on a Micromeritics Autopore 9220. Raman spectra were recorded on an EQUINOX 55 spectrometer equipped with a FT-Raman accessory FRA 160/S (Bruker optics) in backscattering mode. Differential thermal analysis was performed on a Linseis TG/STA-PT1600 thermoanalyser coupled to a mass spectrometer (Balzers, Quadstar).

1 A. Macfarlane and G. Martin, *Science*, 2004, **305**, 1407–8.
2 T. Rehren and E. B. Pusch, *Science*, 2005, **308**, 1756–8.
3 J. E. Shelby, *Introduction to Glass Science and Technology*, Royal Society of Chemistry, Cambridge, 1997.
4 D. R. Uhlmann and N. J. Kreidl, *Optical Properties of Glass*, American Ceramic Society, Westerville, OH, 1991.
5 A. Paul, *J. Mater. Sci.*, 1977, **12**, 2246–68.
6 S. Takahashi, *Adv. Mater.*, 1993, **5**, 187–91.
7 R. D. Maurer, *IEEE Proceedings*, 1973, **61**, 452–62.
8 J. K. R. Weber, J. J. Felten, B. Cho and P. C. Nordine, *Nature*, 1998, **393**, 769–71.
9 L. L. Hench, R. J. Splinter, W. C. Allen and T. K. Greenlee, *J. Biomed. Mater. Res.*, 1971, **5**, 117–41.
10 L. L. Hench and J. Wilson, *Science*, 1984, **226**, 630–6.
11 T. Nakamura, T. Yamamuro, S. Higashi, T. Kokubo and S. Itoo, *J. Biomed. Mater. Res.*, 1985, **19**, 685–98.
12 H. Oonishi, S. Kushitani, E. Yasukawa, H. Iwaki, L. L. Hench, J. Wilson, E. Tsuji and T. Sugihara, *Clin. Orthop. Relat. Res.*, 1997, 316–25.
13 L. L. Hench and J. Wilson, *An Introduction to Ceramics*, World Scientific, Singapore, 1993.
14 B. L. Cushing, V. L. Kolesnichenko and C. J. O'Connor, *Chem. Rev.*, 2004, **104**, 3893–946.
15 C. J. Brinker and G. W. Sherer, *J. Non-Cryst. Solids*, 1985, **70**, 301–22.
16 S. Klein, S. Thorimbert and W. F. Maier, *J. Catal.*, 1996, **163**, 476–88.
17 R. Roy, *Science*, 1987, **238**, 1664–9.
18 L. L. Hench and J. K. West, *Chem. Rev.*, 1990, **90**, 33–72.
19 R. N. Grass and W. J. Stark, *Chem. Commun.*, 2005, 1767–9.
20 S. Loher, W. J. Stark, M. Maciejewski, A. Baiker, S. E. Pratsinis, D. Reichardt, F. Maspero, F. Krumeich and D. Gunther, *Chem. Mater.*, 2005, **17**, 36–42.
21 F. E. Wagner, S. Haslbeck, L. Stievano, S. Calogero, Q. A. Pankhurst and P. Martinek, *Nature*, 2000, **407**, 691–2.
22 L. Mädler, H. K. Kammler, R. Mueller and S. E. Pratsinis, *J. Aerosol Sci.*, 2002, **33**, 369–89.
23 A. Paul and R. W. Douglas, *Phys. Chem. Glasses*, 1969, **10**, 133–8.
24 H. Yamamoto, T. Naito, M. Terao and T. Shintani, *Thin Solid Films*, 2002, **411**, 289–97.
25 L. Madler, W. J. Stark and S. E. Pratsinis, *J. Mater. Res.*, 2003, **18**, 115–20.
26 H. A. ElBatal, M. A. Azooz, E. M. A. Khalil, A. S. Monem and Y. M. Hamdy, *Mater. Chem. Phys.*, 2003, **80**, 599–609.
27 Y. S. Lin, I. Kumakiri, B. N. Nair and H. Alsyouri, *Separ. Purif. Methods*, 2002, **31**, 229–379.
28 K. Kuraoka, T. Hirano and T. Yazawa, *Chem. Commun.*, 2002, 664–5.
29 S. Radin, S. Falaize, M. H. Lee and P. Ducheyne, *Biomaterials*, 2002, **23**, 3113–22.
30 T. Kokubo, H. Kushitani, S. Sakka, T. Kitsugi and T. Yamamuro, *J. Biomed. Mater. Res.*, 1990, **24**, 721–34.
31 I. Notingher, A. R. Boccaccini, J. Jones, V. Maquet and L. L. Hench, *Mater. Charact.*, 2002, **49**, 255–60.
32 D. Gunther, R. Frischknecht, C. A. Heinrich and H. J. Kahlert, *J. Anal. At. Spectrom.*, 1997, **12**, 939–44.

